Decadal-to-Centennial Modulation of ENSO in the GFDL CM2.1 Coupled GCM

Andrew T. Wittenberg

NOAA Geophysical Fluid Dynamics Laboratory, Princeton, New Jersey, USA

A pre-industrial control simulation of the GFDL CM2.1 global coupled GCM, run for 2000 years with its atmospheric composition, solar irradiance, and land cover held fixed at 1860 values, exhibits strong interdecadal and intercentennial modulation of its ENSO behavior. To the extent that such modulation is realistic, it could attach large uncertainties to ENSO metrics diagnosed from centennial and shorter records – with important implications for historical and paleo records, climate projections, and model assessment and intercomparison. An analysis of ENSO inter-event wait times suggests that this long-term modulation need not require multidecadal memory; it can arise simply from Poisson statistics applied to the interannual memory associated with ENSO and its seasonal phase-locking.

1. Introduction

The El Niño/Southern Oscillation (ENSO) is Earth's dominant interannual climate fluctuation, affecting agriculture, ecosystems, and weather around the globe. Yet there remains substantial uncertainty about the future behavior of ENSO, with a wide diversity of model projections for the 21st century [*Guilyardi et al.*, 2009], and even the past behavior of ENSO is not fully understood. Historical SST reconstructions (e.g. Fig. 1a) indicate multidecadal variations in ENSO behavior, but these extend only back to the mid-19th century and must cope with sparse and changing observing systems. Paleoproxy records – such as corals, lake sediments, and tree rings – also suggest past modulation of ENSO (see *Cane* [2005] for a review), but these remain limited in their spatial and temporal sampling, and in some cases could confound changes in ENSO with changes in local climate or ENSO's teleconnections to proxy sites.

Climate models could also potentially shed light on long-term variations in ENSO. Simple and intermediate-complexity ENSO models have long been capable of producing irregular ENSOs [*Zebiak and Cane*, 1987; *Cane et al.*, 1995; *Wittenberg*, 2002; *Timmermann et al.*, 2003; *An et al.*, 2008; *Kleeman*, 2008; *Fang et al.*, 2008], as have coarse-resolution and flux-adjusted coupled GCMs (CGCMs) [*Knutson et al.*, 1997; *Timmermann et al.*, 1999; *Yukimoto and Kitamura*, 2003; *Min et al.*, 2005; *Brown et al.*, 2008]. However, only recently have available computer power and model codes permitted CGCMs with fairly realistic ENSOs to run for millennia, without flux adjustments and with little climate drift.

The dearth of long ENSO records from observations and CGCMs leaves key questions unanswered. In the absence of external perturbations, what is the likelihood of extended epochs of very strong or weak ENSO variations? What causes these epochs, and are they predictable? How long a record is needed to distinguish an ENSO simulation from observations or another simulation, or to discern impacts of a change in physical parameters or climate forcings?

Here we present a CGCM simulation that exhibits very slow modulation time scales for ENSO. While our immediate goal is to describe this model's sampling variability – for later use in detecting impacts of climate forcings and model development – our broader objective is to spur the climate community to consider long-term modulation of ENSO in other models, observations, and paleoclimate records.

0094-8276/09/$5.00

2. Experiment

The Geophysical Fluid Dynamics Laboratory (GFDL) CM2.1 global coupled atmosphere/ocean/land/ice GCM is described by *Delworth et al.* [2006] and references therein. CM2.1 played a prominent role in the third Coupled Model Intercomparison Project (CMIP3) and the Fourth Assessment of the Intergovernmental Panel on Climate Change (IPCC), and its tropical and ENSO simulations have consistently ranked among the world's top GCMs [*van Oldenborgh et al.*, 2005; *Wittenberg et al.*, 2006; *Guilyardi*, 2006; *Joseph and Nigam*, 2006; *Reichler and Kim*, 2008]. The coupled pre-industrial control run is initialized as in *Delworth et al.* [2006], and then integrated for 2220 yr with fixed 1860 estimates of solar irradiance, land cover, and atmospheric composition; we focus here on just the last 2000 yr. This represents a major computing resource investment, requiring over one full year to run on 60 processors at GFDL.

3. Results

3.1. NINO3 SST time series

Fig. 1b shows the resulting 20 centuries of simulated pre-industrial SSTs, averaged over the NINO3 region (150°W-90°W, 5°S-5°N) in the heart of the interannual SST variability in both CM2.1 and the observations. CM2.1, which runs without flux adjustments, produces very little drift in its simulated NINO3 time-mean SST: the second millennium is only 0.1°C warmer than the first. The simulated 2000 yr mean is slightly cooler than observed over 1876–1975, due to both the absence of increasing greenhouse gases in the control run, and a CM2.1 cold bias evident even in 20th-century simulations [*Wittenberg et al.*, 2006].

The modulation of the CM2.1 ENSO is striking. There are multidecadal epochs with hardly any variability (M5); epochs with intense, warm-skewed ENSO events spaced five or more years apart (M7); epochs with moderate, nearly sinusoidal ENSO events spaced three years apart (M2); and epochs that are highly irregular in amplitude and period (M6). One can even find multidecadal epochs where the simulation mimics (by chance) the detailed temporal sequences of observed ENSO events; in both R2 and M6, there are decades of weak, biennial oscillations, followed by a large warm event, then several smaller events, another large warm event, and then a long quiet period. Although the model's NINO3 SST variations are generally stronger than observed, there are long epochs (like M1) where the ENSO amplitude agrees well with observations (R1). An unlucky modeler – who by chance had witnessed only M1-like variability

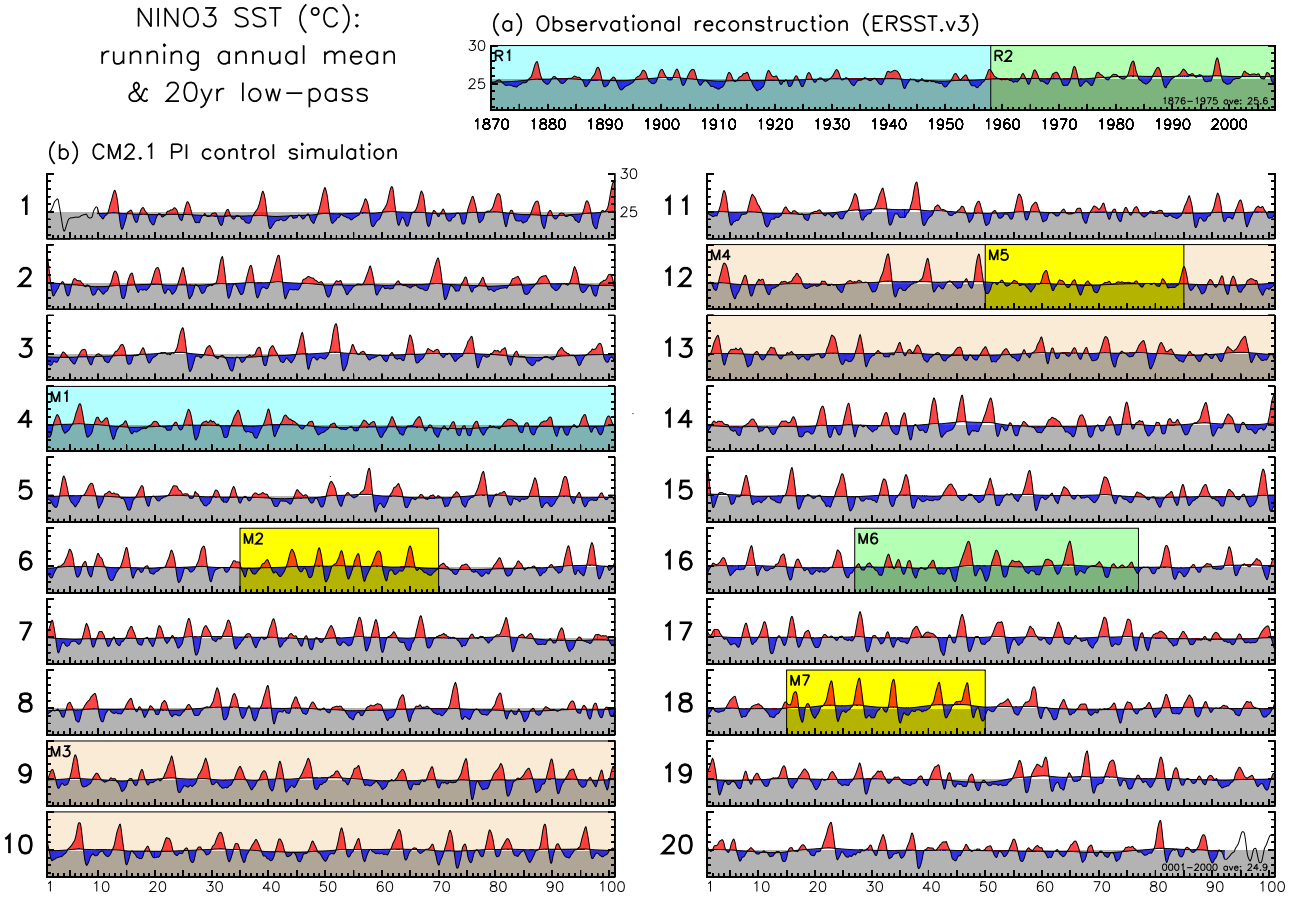

Figure 1. SST (°C) averaged over the NINO3 region (150°W-90°W, 5°S-5°N), for (a) the ERSST.v3 historical reconstruction of *Smith et al.* [2008], and (b) the 20 consecutive centuries (numbered) from the CM2.1 pre-industrial control run. Red/blue shading highlights departures of the running annual-mean SST from the multidecadal background state, where the latter is obtained via a 211-month triangle smoother which transmits (25, 50, 75)% of the timeseries amplitude at periods of (15, 20, 30) yr. Ends of the observed time series in (a) are zero-padded prior to smoothing. The top of the gray bar corresponds to a long-term mean, indicated at the bottom right of each panel. Labeled epochs are discussed in the text.

throughout the first century of simulation – might have erroneously inferred that the model's ENSO amplitude matched the observed record, when in fact a longer simulation would have revealed a much stronger model ENSO.

If the real-world ENSO is similarly modulated, then there is a more disturbing possibility. Had the research community been unlucky enough to observe an unrepresentative ENSO over the past 150 yr of measurements, then it might collectively have misjudged ENSO's longer-term natural behavior. In that case, historically-observed statistics could be a poor guide for modelers, and observed "trends" in ENSO statistics might simply reflect natural variations – as opposed to fundamental, nonstationary changes in ENSO mechanism.

The modulation time scales of the CM2.1 ENSO are surprisingly long. A 200 yr epoch of consistently strong variability (M3) can be followed, just one century later, by a 200 yr epoch of weak variability (M4). Documenting the intercentennial extremes in such a system might thus require a 500+ yr record. Yet few modeling centers currently attempt simulations of that length when evaluating CGCMs under development – due to competing demands for high model resolution, process completeness, and fast turnaround to permit exploration of model sensitivities. Thus a model development team might not even recognize a simulation that manifested long-term ENSO modulation, until after freezing model development and completing long production runs. Clearly, such long-term modulation could hinder progress in ENSO modeling. An unlucky modeler – unaware of the centennial sampling variability in ENSO – could be misled by comparisons of short, unrepresentative model runs, perhaps erroneously rejecting an improved model or erroneously accepting a degraded model.

3.2. Distribution of NINO3 spectra

Fig. 2 shows the time-mean spectrum of the CM2.1 ENSO, for non-overlapping epochs of various lengths. For 20 yr time series – roughly the duration of observations from satellites and the Tropical Atmosphere Ocean (TAO) buoy array – there are large departures of the sample spectra from the true long-term mean spectrum. For century-long time series – near the limit of historical SST reconstructions like that in Fig. 1a – the inter-epoch spread of spectra is reduced by a factor of about $(100/20)^{1/2} = 2.2$ compared to the 20 yr spectra, as expected for independent estimates of the spectrum. Yet there remains a large spread among centennial

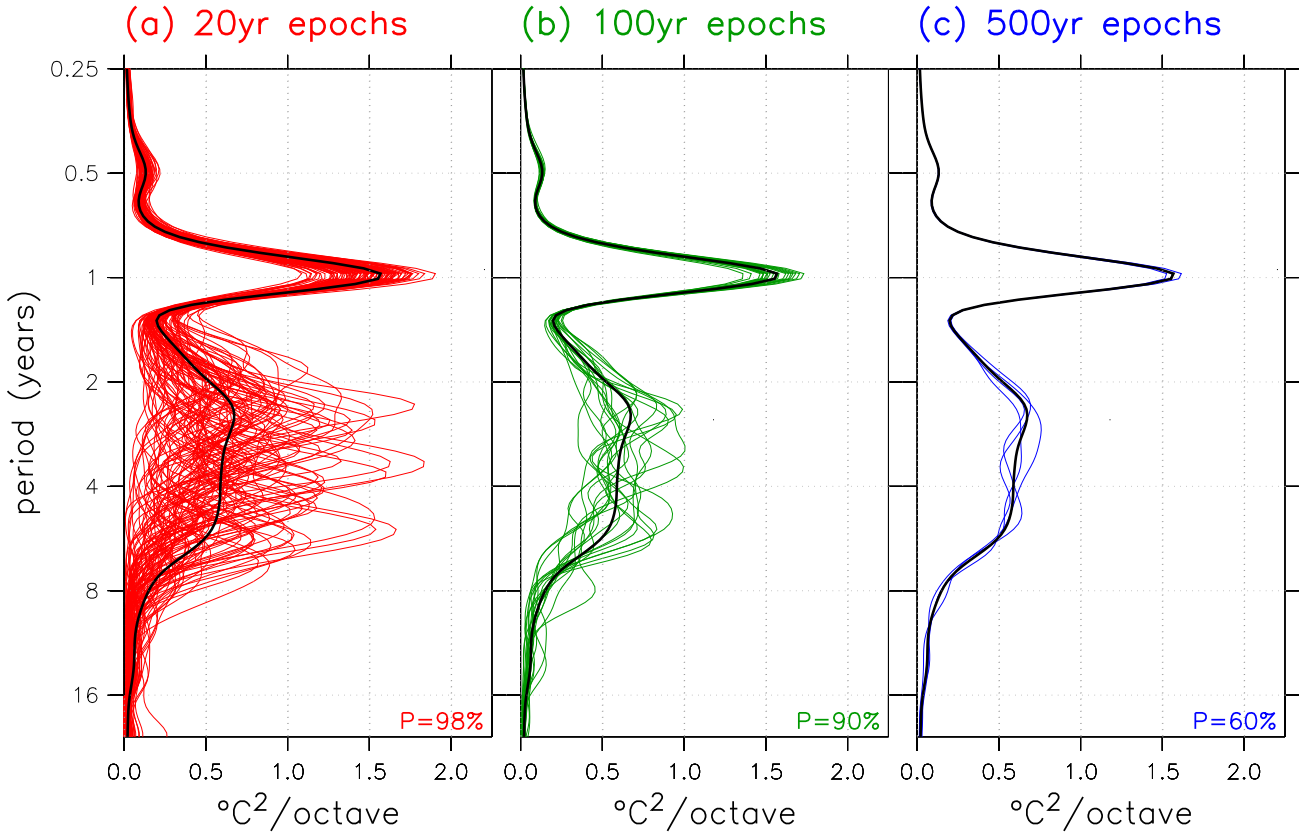

Figure 2. Power spectra of NINO3-averaged SSTs from CM2.1, as a function of the period in octaves of the annual cycle. These spectra, computed by time-averaging the spectral power density from a Morlet wavenumber-6 wavelet analysis, are energy-preserving in that the area to the left of each curve gives the total spectral power within any frequency band. The thick black line is the average spectrum for the full 2000 yr run; thin colored lines are the N subspectra from non-overlapping epochs of length (a) 20 yr ($N = 100$), (b) 100 yr ($N = 20$), and (c) 500 yr ($N = 4$). Were the subspectra independent and identically distributed, the extrema of the N subspectra at each time scale would comprise a prediction interval for the next subspectrum; at bottom right is the probability $P = (N-1)/(N+1)$ that an interval so constructed would bracket the next subspectrum to emerge from the model.

spectra, as the extremes (which comprise a 90% prediction interval for the next centennial spectrum) still span a factor of 2 in power in the interannual band. Only for epochs of 500 yr or more does the sampling variability fall to a small fraction of the total interannual power.

3.3. Inter-event wait times

As in nature, CM2.1 ENSO warm events are stronger and peak farther east than cold events – producing a residual time-mean SST that is warm in the east Pacific and cold in the west during active-ENSO epochs. This residual is evident in NINO3 during active decadal epochs like M7 in Fig. 1; a similar rectification mechanism has been identified as a source of decadal-scale SST variations in the Pacific [*Jin et al.*, 2003; *Rodgers et al.*, 2004; *Schopf and Burgman*, 2006]. But at centennial time scales the CM2.1 tropical Pacific shows little change in mean SST, e.g. between the active (M3) and inactive (M4) epochs of Fig. 1. The largest centennial-mean differences are in the western equatorial Pacific, where compared to M4, the active M3 epoch is cooler by just 0.3°C in SST and 0.1°C averaged over the top 300 m (not shown). While it seems unlikely that such small changes could cause the large centennial variations in CM2.1's ENSO, we shall not attempt to resolve this here. Rather, we ask whether the long-term modulation could arise spontaneously from nothing more than ENSO's interannual time scale. To this end, it proves illuminating to explore the statistics of the wait times between ENSO warm events.

The CM2.1 inter-event wait times are determined as follows. A monthly climatology is removed from the 2000 yr time series of NINO3 SSTs, and the resulting anomalies are smoothed with an 11-month triangle smoother that transmits (25, 50, 75)% of the timeseries amplitude at periods of (0.8, 1.1, 1.7) yr. The resulting time series is then searched for warm events that exceed one standard deviation (1.1°C) for at least 4 months. For each of the 250 such warm events, we then record the month of peak warm anomaly, and the time to the next warm event peak.

The resulting distribution of wait times is plotted in Fig. 3. For comparison, we overlay the corresponding distributions for a memoryless (Poisson) process with the same mean wait $\overline{\tau}$ as in CM2.1. The Poisson wait times are exponentially distributed; their cumulative distribution

$$P\,(wait < \tau) = 1 - e^{-\tau/\overline{\tau}} \qquad (1)$$

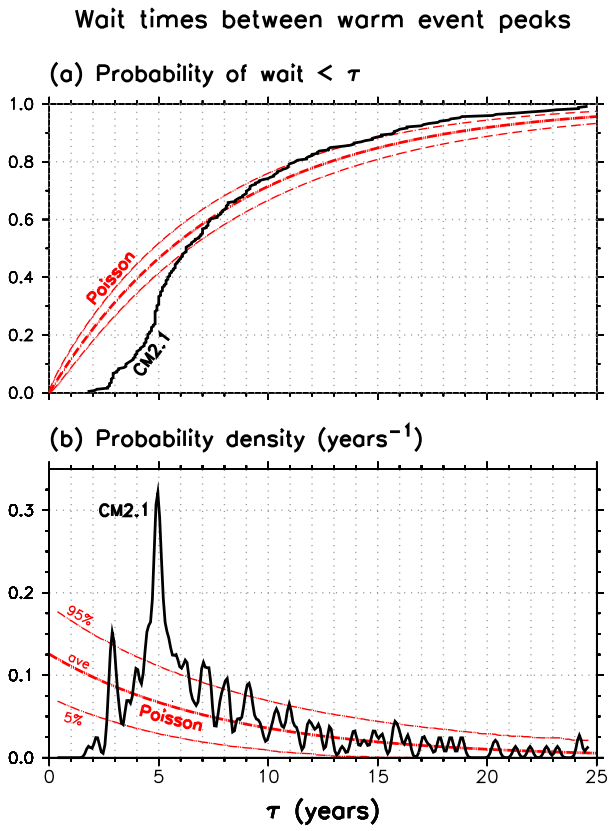

Figure 3. Distribution of wait times between warm event peaks, for CM2.1 (black line) and a Poisson process with CM2.1's average wait time of 8 yr (red lines). (a) Probability that wait time does not exceed time τ; (b) probability density of wait times, smoothed using a Gaussian kernel with a 2-month e-folding halfwidth. Poisson percentiles are computed from 100,000 Monte Carlo realizations of 250 Poisson events, processed just like the 250 CM2.1 events.

and probability density

$$p(\tau) = \frac{1}{\overline{\tau}} e^{-\tau/\overline{\tau}} \qquad (2)$$

are plotted as the central red line. The outer red lines comprise a central 90% confidence interval, obtained from repeated samples of 250 simulated Poisson events (the same number of warm events found in Fig. 1b).

The CM2.1 wait distribution is highly skewed, with a mode of 5 yr, a median of 6 yr, and a mean wait of $\overline{\tau} = 8$ yr. In contrast to the Poisson events, the CM2.1 events occur no less than 1.3 yr apart – due to the slow recharge of west Pacific warm pool heat content via off-equatorial Sverdrup adjustment and gradual surface-flux heating [*Jin*, 1996; *Yukimoto and Kitamura*, 2003]. CM2.1 also clearly favors an integral number of years between events – due to the seasonal phase-locking of ENSO, and reminiscent of the quasi-periodicity seen in simple and intermediate-complexity ENSO models [*Jin et al.*, 1994; *Tziperman et al.*, 1995].

The CM2.1 annual peaks at 3, 5, 7, 8, and 9 yr all exceed the Poisson 95% limits, suggesting that NINO3 SST may retain some memory of past warm events for up to a decade. But beyond 10 yr, the CM2.1 wait times are statistically indistinguishable from a Poisson process – there is no evidence of inter-event memory in CM2.1 NINO3 SSTs at multidecadal time scales. Yet 15% of the Poisson events, and 10% of the CM2.1 warm events, occur more than 15 yr after their predecessors, and waits of nearly 25 yr can be found in CM2.1. Thus even a memoryless interannual process can occasionally produce very long wait times between El Niños, resulting in apparent ENSO modulation.

4. Summary and Discussion

A pre-industrial control simulation of the GFDL CM2.1 global coupled GCM, run for 2000 yr with its atmospheric composition, solar irradiance, and land cover held fixed at 1860 values, exhibits strong interdecadal and intercentennial modulation of its ENSO behavior. This sampling variability attaches large uncertainties to certain ENSO metrics – such as the NINO3 SST variance and spectrum – diagnosed from centennial and shorter records. A null hypothesis for the slow modulation is that it arises from Poisson statistics applied to interannual memory, the latter associated with ENSO's seasonal phase-locking, delayed recharge, and modal time scales. This hypothesis must ultimately be weighed against alternatives – e.g. that separate decadal climate modes alter ENSO stability, that ENSO acts to regulate the tropical climatology, or that past ENSO modulation has resulted from orbital or anthropogenic forcings.

Toward the IPCC Fifth Assessment, GFDL has developed several new CGCMs (CM2M, CM2G, and CM3), each of which uses either a different atmosphere or a different ocean from CM2.1. Preliminary control runs from these models also exhibit centennial-scale modulation of ENSO, as does a 700 yr run from the NCAR CCSM3.5 CGCM (B. Fox-Kemper, personal communication, 2008). If this is the case with other CGCMs – such as those in the CMIP3 archive – then model evaluation and intercomparison might require large ensembles or long runs (5 centuries or more) to expose robust changes in ENSO. More worryingly, if nature's ENSO is similarly modulated, there is no guarantee that the 150 yr historical SST record is a fully representative target for model development.

The climate community could meet these challenges in several ways. Longer and more densely-sampled paleo records could illuminate the behavior of ENSO farther back in time. More extreme tests of climate models – e.g. under mid-Holocene or glacial conditions – could produce larger ENSO changes that are more detectable in the face of sampling uncertainty. Alternate ENSO metrics – such as regressions scaled by ENSO amplitude – could highlight mechanisms with less sampling variability than that associated with ENSO spectra and variances.

That internally-generated modulation of ENSO may exist even with fixed climate forcings, does not preclude additional impacts of external perturbations – like orbital variations and anthropogenic forcings – which have been demonstrated to affect ENSO in climate models [*Guilyardi et al.*, 2009]; internally-generated modulation simply makes it more challenging to detect these effects. In any case, it is sobering to think that even absent any anthropogenic changes, the future of ENSO could look very different from what we have seen so far.

Acknowledgments. The author is grateful to A. Rosati, T. Knutson, G. Vecchi, S. Griffies, and F.-F. Jin for their helpful comments.

References

An, S.-I., J.-S. Kug, Y.-G. Ham, and I.-S. Kang (2008), Successive modulation of ENSO to the future greenhouse warming, *J. Climate*, *21*, 3–21.

Brown, J., M. Collins, A. W. Tudhope, and T. Toniazzo (2008), Modelling mid-Holocene tropical climate and ENSO variability: Towards constraining predictions of future change with palaeo-data, *Climate Dyn.*, *30*, 19–36.

Cane, M. A. (2005), The evolution of El Niño, past and future, *Earth Plane. Sci. Lett.*, *230*, 227–240.

Cane, M. A., S. E. Zebiak, and Y. Xue (1995), Model studies of the long-term behavior of ENSO, in *Natural Climate Variability on Decade-to-Century Time Scales*, pp. 442–457, National Academy Press.

Delworth, T. L., A. J. Broccoli, A. Rosati, R. J. Stouffer, and Coauthors (2006), GFDL's CM2 global coupled climate models, Part I: Formulation and simulation characteristics, *J. Climate*, *19*, 643–674.

Fang, Y., J. C. H. Chiang, and P. Chang (2008), Variation of mean sea surface temperature and modulation of El Niño-Southern Oscillation variance during the past 150 years, *Geophys. Res. Lett.*, *35*, L14,709, doi:10.1029/2008GL033761.

Guilyardi, E. (2006), El Niño-mean state-seasonal cycle interactions in a multi-model ensemble, *Climate Dyn.*, *26*, 329–348.

Guilyardi, E., A. Wittenberg, A. Fedorov, M. Collins, C. Wang, A. Capotondi, G. J. van Oldenborgh, and T. Stockdale (2009), Understanding El Niño in ocean-atmosphere general circulation models: Progress and challenges, *Bull. Amer. Meteor. Soc.*, *90*, 325–340.

Jin, F.-F. (1996), Tropical ocean-atmosphere interaction, the Pacific cold tongue, and the El Niño-Southern Oscillation, *Science*, *274*, 76–78.

Jin, F.-F., J. D. Neelin, and M. Ghil (1994), El Niño on the devil's staircase: Annual subharmonic steps to chaos, *Science*, *264*, 70–72.

Jin, F.-F., S.-I. An, A. Timmermann, and J. Zhao (2003), Strong El Niño events and nonlinear dynamical heating, *Geophys. Res. Lett.*, *30*, 1120, doi:10.1029/2002GL016356.

Joseph, R., and S. Nigam (2006), ENSO evolution and teleconnections in IPCC's twentieth-century climate simulations: Realistic representation?, *J. Climate*, *19*, 4360–4377.

Kleeman, R. (2008), Stochastic theories for the irregularity of ENSO, *Phil. Trans. Roy. Soc. A*, *366*, 2511–2526.

Knutson, T. R., S. Manabe, and D. Gu (1997), Simulated ENSO in a global coupled ocean-atmosphere model: Multidecadal amplitude modulation and CO_2 sensitivity, *J. Climate*, *10*, 138–161.

Min, S.-K., S. Legutke, A. Hense, and W.-T. Kwon (2005), Internal variability in a 1000-yr control simulation with the coupled climate model ECHO-G. II. El Niño Southern Oscillation and North Atlantic Oscillation, *Tellus*, *57A*, 622–640.

Reichler, T., and J. Kim (2008), How well do coupled models simulate today's climate?, *Bull. Amer. Meteor. Soc.*, *89*, 303–311.

Rodgers, K. B., P. Friederichs, and M. Latif (2004), Tropical Pacific decadal variability and its relation to decadal modulations of ENSO, *J. Climate*, *17*, 3761–3774.

Schopf, P. S., and R. J. Burgman (2006), A simple mechanism for ENSO residuals and asymmetry, *J. Climate*, *19*, 3167–3179.

Smith, T. M., R. W. Reynolds, T. C. Peterson, and J. Lawrimore (2008), Improvements to NOAA's historical merged land-ocean surface temperature analysis (1880-2006), *J. Climate*, *21*, 2283–2296.

Timmermann, A., J. Oberhuber, A. Bacher, M. Esch, M. Latif, and E. Roeckner (1999), Increased El Niño frequency in a climate model forced by future greenhouse warming, *Nature*, *398*, 694–697.

Timmermann, A., F.-F. Jin, and J. Abshagen (2003), A nonlinear theory for El Niño bursting, *J. Atmos. Sci.*, *60*, 152–165.

Tziperman, E., M. A. Cane, and S. E. Zebiak (1995), Irregularity and locking to the seasonal cycle in an ENSO prediction model as explained by the quasi-periodicity route to chaos, *J. Atmos. Sci.*, *52*, 293–306.

van Oldenborgh, G. J., S. Y. Philip, and M. Collins (2005), El Niño in a changing climate: A multi-model study, *Ocean Science*, *1*, 81–95.

Wittenberg, A. T. (2002), ENSO Response to Altered Climates, Ph.D. thesis, Princeton University, 475pp.

Wittenberg, A. T., A. Rosati, N.-C. Lau, and J. J. Ploshay (2006), GFDL's CM2 global coupled climate models. Part III: Tropical Pacific climate and ENSO, *J. Climate*, *19*, 698–722.

Yukimoto, S., and Y. Kitamura (2003), An investigation of the irregularity of El Nino in a coupled GCM, *J. Meteor. Soc. Japan*, *81*, 599–622.

Zebiak, S. E., and M. A. Cane (1987), A model El Niño-Southern Oscillation, *Mon. Wea. Rev.*, *115*, 2262–2278.

A. T. Wittenberg, NOAA Geophysical Fluid Dynamics Laboratory, US DOC/GFDL, P.O. Box 308, 201 Forrestal Road, Forrestal Campus, US Route 1, Princeton, NJ 08542-0308, USA. (andrew.wittenberg@noaa.gov)